HHS Public Access

Author manuscript

Oncogene. Author manuscript; available in PMC 2015 November 07.

Published in final edited form as:

Oncogene. 2015 May 7; 34(19): 2471–2482. doi:10.1038/onc.2014.193.

Loss of *Cdh1* and *Trp53* in the uterus induces chronic inflammation with modification of tumor microenvironment

Genna R. Stodden[1], **Mallory E. Lindberg**[1], **Mandy L. King**[1], **Marilène Paquet**[2], **James A. MacLean II**[1], **Jordan L. Mann**[3], **Francesco J. DeMayo**[4], **John P. Lydon**[4], and **Kanako Hayashi**[1]

[1]Department of Physiology, Southern Illinois University School of Medicine, Carbondale, IL, USA

[2]Departement de Pathologie et de Microbiologie, Université de Montreal, St-Hyacinthe (Qc) J2S 2M2, Canada

[3]Department of Pathology, Southern Illinois University School of Medicine, Springfield, IL, USA

[4]Department of Molecular and Cellular Biology, Baylor College of Medicine, Houston TX, USA

Abstract

Type II endometrial carcinomas are estrogen independent, poorly differentiated tumors that behave in an aggressive manner. Since *TP53* mutation and CDH1 inactivation occur in 80% of human endometrial type II carcinomas, we hypothesized that mouse uteri lacking both *Trp53* and *Cdh1* would exhibit a phenotype indicative of neoplastic transformation. Mice with conditional ablation of *Cdh1* and *Trp53* (*Cdh1*$^{d/d}$*Trp53*$^{d/d}$) clearly demonstrate architectural features characteristic of type II endometrial carcinomas, including focal areas of papillary differentiation, protruding cytoplasm into the lumen (hobnailing) and severe nuclear atypia at 6-mo of age. Further, *Cdh1*$^{d/d}$*Trp53*$^{d/d}$ tumors in 12-mo old mice were highly aggressive, and metastasized to nearby and distant organs within the peritoneal cavity, such as abdominal lymph nodes, mesentery and peri-intestinal adipose tissues, demonstrating that tumorigenesis in this model proceeds through the universally recognized morphologic intermediates associated with type II endometrial neoplasia. We also observed abundant cell proliferation and complex angiogenesis in the uteri of *Cdh1*$^{d/d}$*Trp53*$^{d/d}$ mice. Our microarray analysis found that most of the genes differentially regulated in the uteri of *Cdh1*$^{d/d}$*Trp53*$^{d/d}$ mice were involved in inflammatory responses. CD163 and *Arg1*, markers for tumor-associated macrophages, were also detected and increased in the uteri of *Cdh1*$^{d/d}$*Trp53*$^{d/d}$ mice, suggesting that an inflammatory tumor microenvironment with immune cell recruitment is augmenting tumor development in *Cdh1*$^{d/d}$*Trp53*$^{d/d}$ uteri. Further, inflammatory mediators secreted from CDH1 negative, *TP53* mutant endometrial cancer cells induced normal macrophages to express inflammatory related genes through activation of NFκB

Correspondence: Kanako Hayashi, Department of Physiology, Southern Illinois University School of Medicine, 1135 Lincoln Dr. Carbondale, IL 62901, khayashi@siumed.edu.
GRS and MEL contributed equally to this work.

CONFLICT OF INTEREST

The authors declare no conflict of interest.

No potential conflicts of interest were declared.

signaling. These results indicate that absence of CDH1 and TP53 in endometrial cells initiates chronic inflammation, promotes tumor microenvironment development following the recruitment of macrophages, and promotes aggressive endometrial carcinomas.

Keywords

CDH1; TRP53; inflammation; endometrial cancer; uterus

INTRODUCTION

Endometrial cancer is the most common malignancy of the female genital tract, affecting over 52,000 women and leading to approximately 8,500 deaths in the US each year.[1] Two types of endometrial carcinomas (ECs) have been distinguished, type I (T1EC) and type II (T2EC).[2] T1ECs, which account for 80% of all ECs, are associated with hyperestrogenism, have a good prognosis, exhibit atypical hyperplasia, and usually develop in pre- and peri-menopausal women.[3, 4] T2ECs are high-grade, estrogen-independent, and diagnosed mainly in post-menopausal women. Although only 15–20% of ECs belong to T2ECs, these tumors appear to be very aggressive, and more than 50% of patients present with recurrent disease shortly after primary treatment.[5–7] Further, less than 30% of the patients with T2ECs survive 5 years after initial diagnosis.[5] Therefore, a clear understanding of the mechanisms involved in tumor development of T2ECs is necessary for early stage diagnosis as well as rational design of therapies.

T2ECs are poorly differentiated, aggressive tumors.[8–10] The most common histological tumor type is serous carcinoma comprised of atypical cells that grow into papillary, glandular or solid tumors.[8, 9, 11] A number of studies have reported that *TP53* mutations are associated with poor prognosis.[4, 8, 12] Inactivation of TP53 renders cells non-responsive to signals that challenge genomic integrity, thereby promoting the acquisition of novel and harmful cellular phenotypes that are characteristic of cancer cells, such as resistance to apoptosis, neoangiogenesis, and enhanced proliferative and invasive potential. Approximately 80% of T2ECs harbor *TP53* mutations. Although *TP53* mutations are less common in T1ECs, those reported have been largely confined to high grade tumors (grade 3 and 4).[8] In addition to *TP53* mutation, inactivation of CDH1 is also a common molecular feature in T2ECs.[4, 10] CDH1 is critical in the establishment of cell polarity and maintenance of the epithelial phenotype.[13] CDH1 is often downregulated or lost during tumor progression,[14–17] leading to increased tumor invasiveness and metastasis.[4, 18–22]

Mice with either *Trp53* heterozygous or homozygous deletion develop a variety of cancers with most homozygous mice dying by 6-mo due to development of widespread lymphoma, but *Trp53*-null mice rarely form ECs.[23–25] $Pgr^{Cre/+}$ mice have been recognized as an excellent model to target genes in the uterus after birth.[26] While conditional uterine ablation of *Pten* driven by *Pgr-Cre* results in development of T1ECs in mice,[27, 28] the uteri of mice lacking *Trp53* alone do not exhibit any abnormal morphology by 5-mo.[27] We have recently reported that conditional ablation of *Cdh1* in the mouse uterus results in a disorganized cellular structure of the epithelium and ablation of endometrial glands, leading to

implantation defects.[29] However, loss of *Cdh1* alone in the uterus does not predispose mice to tumors. Conditional ablation of *Cdh1* does not induce tumors in mammary glands[30–32] or stomach,[33] whereas loss of *Cdh1* and *Trp53* induces invasive lobular carcinoma in mammary glands with massive angiogenesis.[31, 32] Thus, these results indicate that single gene ablation in the uterus is not sufficient to understand the etiology of heterogeneous aggressive types of ECs.

In the present study, we generated a mouse model in which *Cdh1* and *Trp53* were conditionally ablated in the uterus. Ablation of *Trp53* and *Cdh1* accelerated endometrial neoplastic transformation and induced cell invasion and dissemination. Further, the results of the present study suggest that ablation of *Cdh1* and *Trp53* in the mouse uterus initiates chronic inflammation with tumor microenvironment modification which promotes aggressive ECs.

RESULTS

Generation of mice with Cdh1 and Trp53 ablation in the mouse uterus

Because *TP53* mutation and CDH1 inactivation are the two most common found molecular features in human T2ECs,[3, 4] our objective was to study the combined effect of dysfunctional uterine TRP53 and CDH1. As *Cdh1*-null mice show early embryonic lethality,[34, 35] we conditionally deleted both *Cdh1* and *Trp53* in the uterus using $Pgr^{Cre/+}$ mice. $Pgr^{Cre/+}$ mice were crossed with $Cdh1^{f/f}$ and/or $Trp53^{f/f}$ mice to provide a tissue-specific knockout of *Cdh1* and/or *Trp53* in *Pgr*-expressing cells: $Pgr^{+/+}Cdh1^{f/f}Trp53^{f/f}$ = control, $Pgr^{Cre/+}Cdh1^{f/f}Trp53^{+/+} = Cdh1^{d/d}$, $Pgr^{Cre/+}Cdh1^{+/+}Trp53^{f/f} = Trp53^{d/d}$, $Pgr^{Cre/+}Cdh1^{f/f}Trp53^{f/+} = Cdh1^{d/d}Trp53^{d/+}$, $Pgr^{Cre/+}Cdh1^{f/+}Trp53^{f/f} = Cdh1^{d/+}Trp53^{d/d}$ and $Pgr^{Cre/+}Cdh1^{f/f}Trp53^{f/f} = Cdh1^{d/d}Trp53^{d/d}$ (Supplementary Figure 1). The ability of *Pgr-Cre* to mediate ablation of *Cdh1* and *Trp53* in the uterus was confirmed by CDH1 immunoreactivity and *Trp53* mRNA analysis (Supplementary Figure 1bc). Although Cre recombinase in $Pgr^{Cre/+}$ mice is active in all cell types of the uterus, ablation of both *Cdh1* and *Trp53* in the uterus only occurs in the epithelial cells as endogenous CDH1 is expressed only in the uterine epithelium. While PGR is expressed in the oviduct, ovary, mammary gland and pituitary, we did not see any histological and/or functional abnormalities in other tissues lacking *Cdh1* and *Trp53* (data not shown).

Impact of conditional ablation of Cdh1 and Trp53 in the uterus

Six different genotypes of mice (control, $Cdh1^{d/d}$, $Trp53^{d/d}$, $Cdh1^{d/d}Trp53^{d/+}$, $Cdh1^{d/+}Trp53^{d/d}$ and $Cdh1^{d/d}Trp53^{d/d}$) were generated. While ovarian function in all genotypes was normal, we performed ovariectomy at 6 weeks of age in order to mimic the human disease as T2ECs are estrogen independent and diagnosed mainly in post-menopausal women. Because our first screen in six different genotypes revealed that heterozygous alleles ($Cdh1^{d/d}$ $Trp53^{d/+}$ and $Cdh1^{d/+}Trp53^{d/d}$) did not cause any different phenotypes as demonstrated by uterine gross morphology and histology, survival, and proliferation compared to controls or single gene ablation (Supplementary Figure 2), mice with heterozygous alleles were removed from further analysis. We observed no differences in uterine gross morphology and uterine wet weight between control, $Cdh1^{d/d}$ and $Trp53^{d/d}$

mice at 2-, 6- and 12-mo (Figure 1abci, n=10/genotype/age), as expected. However, *Cdh1*$^{d/d}$*Trp53*$^{d/d}$ mice (n=15/age) exhibited a hyperplastic uterine morphology starting at 6-mo with an increase in uterine wet weight (Figure 1defgi). At 12-mo, all *Cdh1*$^{d/d}$*Trp53*$^{d/d}$ mice developed hyperplastic uterine morphology, and 7 of 15 *Cdh1*$^{d/d}$*Trp53*$^{d/d}$ mice showed migrated tumors through the uterus (Figure 1gh, arrows). We also observed ascites fluid accumulation (4 of 15 mice) starting around 10-mo (Figure 1j). Kaplan-Meier analysis revealed that the survival time of *Cdh1*$^{d/d}$*Trp53*$^{d/d}$ mice was significantly reduced ($P<0.0001$, Figure 1k). Loss of both *Cdh1* and *Trp53* affects survival as early as 5.5-mo, and half of *Cdh1*$^{d/d}$*Trp53*$^{d/d}$ mice died or reached tumor burden euthanasia criteria by 12-mo. While the ovariectomized model is the most appropriate to study T2EC, we also examined mice with intact ovaries (Supplementary Figure 3). We observed massive fluid accumulation in the uterine lumen of *Cdh1*$^{d/d}$, *Cdh1*$^{d/d}$*Trp53*$^{d/+}$ and *Cdh1*$^{d/d}$*Trp53*$^{d/d}$ mice at 6-mo. This phenotype did not affect survival time until 6-mo, but caused thin uterine layers without any carcinogenesis. While estrogen induces engorging of the uterus at estrus, the uterus metabolizes substances/fluids and recovers to normal during the estrous cycle. Our previous study demonstrated that loss of *Cdh1* causes abnormal uterine development and infertility.[29] Thus, loss of *Cdh1* in the uterine epithelium causes abnormal endometrial function and accumulation of fluids in the uterine lumen. Because the intact model did not result in any carcinogenesis, we excluded it from further analysis.

Histological analysis demonstrated that single ablation of either *Trp53* or *Cdh1* in the uterus at 12-mo did not result in any abnormalities (Figure 2abc). In contrast, *Cdh1*$^{d/d}$*Trp53*$^{d/d}$ uteri showed abnormal histology starting at 2-mo, including disorganized epithelium with cellular budding like papillae (Figure 2d) and frequent invasion into myometrium (Figure 2e). Our subsequent studies examining 6- and 12-mo *Cdh1*$^{d/d}$*Trp53*$^{d/d}$ mice revealed poorly differentiated high grade nuclear features with atypia (Figure 2fgh), which are characteristics of T2ECs. Further, tumors exhibited architectural features of T2ECs including focal areas of papillary differentiation (Figure 2i), protruding cytoplasm into the lumen (hobnailing) (Figure 2j), and sarcomatous differentiation (Figure 2k), which is an example of de-differentiation strongly associated with aggressive tumors. Because poor prognosis in T2ECs relates to a propensity for metastasis,[36] we looked at multiple sites in the mice. We observed the first signs of disseminated tumors throughout the peritoneal cavity in *Cdh1*$^{d/d}$*Trp53*$^{d/d}$ mice at 10~12-mo, detecting nodules of tumor growth on the peri-intestinal adipose tissue and mesentery (Figure 2lm), and ECs invading into the mesentery (Figure 2n). Abdominal lymph nodes, especially external iliac nodes, also showed the sign of metastases, which are composed of malignant cells organized in tubular structures (Figure 2o). These results suggest that tumorigenesis in this model proceeds through the recognized morphologic intermediates leading to metastasis associated with T2ECs.[8, 37]

Next, to determine whether an alteration in cell proliferation is occurring in *Cdh1*$^{d/d}$*Trp53*$^{d/d}$ uteri, we performed immunohistochemical staining for Ki67. Nuclear staining of Ki67 in 12-mo uterine sections was analyzed by ImmunoRatio.[38] In agreement with the lack of changes in uterine gross morphology and histology, only a few cells were Ki67 positive in the uteri from control, *Cdh1*$^{d/d}$, *Trp53*$^{d/d}$, *Cdh1*$^{d/d}$ *Trp53*$^{d/+}$, *Cdh1*$^{d/+}$*Trp53*$^{d/d}$ mice, and a significant number of Ki67 positive cells were observed in only the *Cdh1*$^{d/d}$*Trp53*$^{d/d}$ uteri

(Supplementary Figure 2d). Therefore, we focused further analyses to control and *Cdh1*$^{d/d}$*Trp53*$^{d/d}$ mice (Figure 3). The uteri of *Cdh1*$^{d/d}$*Trp53*$^{d/d}$ mice showed significantly increased Ki67 positive cells compared to control uteri, starting at 2-mo (data not shown). Immunostaining of CD31, a marker of endothelial cells, indicated that angiogenesis is more active in *Cdh1*$^{d/d}$*Trp53*$^{d/d}$ uteri than control. Nuclear staining of ESR1 and PGR in different cell types was quantified, and the percentage of positive cells from total cells was shown. Epithelial ESR1 and PGR were decreased following ablation of both *Trp53* and *Cdh1*, although stromal PGR in *Cdh1*$^{d/d}$*Trp53*$^{d/d}$ uteri were increased, suggesting that loss of *Trp53* and *Cdh1* leads to abnormal proliferation, angiogenesis and loss of or abnormal steroid hormone activity.

Chronic inflammation was initiated by ablation of Trp53 and Cdh1

Recent discoveries from both clinical and experimental studies indicate that metastatic progression is an independent process from primary tumor development and acquisition of metastatic competence can occur at an early stage of tumor progression.[39–42] To identify the genetic markers for early tumor development, we performed microarray analysis using the uteri of 2-mo mice following ablation of *Cdh1* and/or *Trp53*. We have deposited this data in the GEO database (GSE48131). Because single ablation of either *Cdh1* or *Trp53* did not cause any tumor formation (Figures 1 and 2), four relevant comparisons were used to identify uterine target genes that are significantly regulated by *Cdh1* and/or *Trp53*. We identified 120 genes that were in common between comparison 3 and 4 (fold-change greater than 2 and FDR $p < 0.05$, Supplementary Figure 4ab). Differentially expressed genes were classified by functional annotation using DAVID analysis[43, 44] and IPA program (Ingenuity Systems, Mountain View, CA). These 120 genes were categorized into groups of inflammatory response (43), immune cell trafficking (38), cell-to-cell signaling and interaction (43), cellular movement (40), cellular growth and proliferation (44), and tissue morphology (39) (Supplementary Figure 4c). The results also revealed that most of the genes overlapped in multiple categories of indicated functional annotations, suggesting that *Cdh1*$^{d/d}$*Trp53*$^{d/d}$ uteri cause inflammation related to aggressive and invasive cell functions. Gene groups were subjected to Gene Set Enrichment Analysis (GSEA) for association of misregulated genes and genetic signatures of various pathways and cellular processes described in the GO, KEGG, Biocarta, and Reactome databases[45]. At an FDR < 20%, 106 gene sets were significantly upregulated following loss of both *Cdh1* and *Trp53* (Supplementary Table 1). In agreement with DAVID and IPA analysis, gene sets related to cytokine signaling, inflammatory responses, cell-cell interaction, and cellular morphology were significantly enriched in *Cdh1*$^{d/d}$*Trp53*$^{d/d}$ uteri. Enrichment plots of representative inflammation pathways show a high degree of correlation in the most upregulated genes within each set and the 120 genes of interest used for DAVID and IPA (Supplementary Figure 5).

Differentially expressed transcripts were confirmed by quantitative RT-PCR (qPCR) and a summary of representative genes (fold change ± SE compared to control) are provided in Figure 4. These results clearly highlighted that many genes, especially those related to inflammation, were upregulated in *Cdh1*$^{d/d}$*Trp53*$^{d/d}$ uteri, but not in single ablation of *Trp53* or *Cdh1* uteri (Figure 4a). Further, identified genes were still at significantly high levels in

Cdh1$^{d/d}$*Trp53*$^{d/d}$ uteri at 12-mo (Figure 4a). Therefore, we speculate that the tumor microenvironment under chronic inflammation represents a central regulator of tumor development leading to cell invasion, dissemination and metastasis. Interestingly, only 4 of 120 genes exhibited decreased expression in *Cdh1*$^{d/d}$*Trp53*$^{d/d}$ uteri.

Additionally, clinically relevant genes differentially expressed between human T1ECs and T2ECs have been identified,[46–48] and gene expression profiles of serous papillary ECs compared to normal endometrium has also been reported.[49] Our model is more similar to that described by Santin et al, thus we also compared our differentially expressed genes to their published data. *Cdkn2a*, *Claudin*, *Interleukin* and *MMP* genes are significantly increased in both women afflicted with this type of ECs and our transgenic mouse model (Figure 4ab and [49]).

Inflammatory signaling within the tumor microenvironment

NFκB and STAT3 are emerging as two key players involved in tumor promotion, progression and metastasis related to inflammation.[50–53] IKKβ-dependent NFκB activation plays a central role in the activation of numerous pro-inflammatory cytokines in multiple cell types including macrophages.[52, 54] Activated NFκB promotes cell proliferation, migration and metastasis by inducing chemokines.[52, 54] Persistent STAT3 activation in malignant cells stimulates cell proliferation, survival, angiogenesis, invasion and tumor-promoting inflammation.[50, 55] STAT3 activation within immune cells enables suppression of anti-tumor immunity and promotes differentiation and recruitment of myeloid cells, specifically tumor associated macrophages (TAM).[50, 55, 56] TAMs are polarized M2 macrophages and are associated with tumor progression, as opposed to the classical macrophages of the M1 phenotype that perform key immune-surveillance and antigen-presentation functions.[57, 58] Therefore, we examined phospho-IKK and phospho-STAT3, as well as known NFκB downstream molecules (COX2 and iNOS), markers for macrophages (CD68) and TAMs (CD163), a known mediator of metastasis (MMP9), as well as phospho-AKT, which is a well-known key player in T1ECs (Figure 5ab).[10, 37] Immunoreactivity of p-IKK, COX2, iNOS, MMP9 and p-AKT was semiquantitatively scored by H-scored analysis.[59] Nuclear staining of p-STAT3 was analyzed by ImmunoRatio.[38] CD68 and CD163 positive cells were manually counted by three independent observers. Significantly increased levels of p-IKK, p-STAT3, CD68, CD163, COX2, iNOS and MMP9, but not p-AKT were observed in *Cdh1*$^{d/d}$*Trp53*$^{d/d}$ uteri. Further, *Arg1*, a commonly accepted M2 marker in mice,[60, 61] was also significantly increased in *Cdh1*$^{d/d}$*Trp53*$^{d/d}$ uteri (Figure 5c). These results suggest that an inflammatory tumor microenvironment with immune cell recruitment is further supporting tumor development in *Cdh1*$^{d/d}$*Trp53*$^{d/d}$ mice. However, activation of AKT signaling is not involved in our model.

EC cells promote the ability of macrophages to stimulate inflammation

Because TAM expression correlates with inflammatory activity in *Cdh1*$^{d/d}$*Trp53*$^{d/d}$ uteri, we investigated inflammatory response between EC cells and macrophages. The activity of NFκB is regulated by interaction with inhibitory IκB proteins. Therefore, we first determined IκB in KLE and AN3CA T2EC cells, RAW264.7 mouse macrophage cells, and RK3E rat epithelial cells as a control. IκB was absent or low abundant in AN3CA or KLE

cells, whereas IκB was positive in RK3E and RAW264.7 cells (Figure 6a). KLE and AN3CA cells were chosen for this study due to the mutation status of *TP53* in both cell lines and absence of CDH1 in AN3CA cells (Figure 6a). When these cells were treated with an NFκB signaling inhibitor, dexamethasone (0, 0.1, 1 or 10 μM) for 24 h, IκB was dose-dependently increased in AN3CA cells, but not in KLE and RK3E cells (Figure 6b), suggesting that AN3CA cells have intact NFκB signaling, but other cells do not. *S100A8* and *IL1B* were the only two factors from our microarray that were detectable in AN3CA cells, and their expression levels were decreased by dexamethasone (Figure 6c). In our mouse model, CD68 and CD163 were positive in $Cdh1^{d/d}Trp53^{d/d}$ uteri (Figure 5). Thus, we hypothesize that interaction of cancer cells and macrophages initiate tumor microenvironment via inflammation and promote tumor growth and progression in ECs. Therefore, we next investigated whether AN3CA-derived factors were able to activate NFκB signaling and stimulate inflammatory related genes in macrophages. We observed that IκB protein was reduced in RAW264.7 cells primed in media conditioned by AN3CA cells (Figure 6d). A dose-dependent increase in IκB was seen in RAW264.7 cells cultured with conditioned media from AN3CA cells that were treated with a dose range of dexamethasone (Figure 6e). Further, genes identified by microarray, *Il1b*, *Ppbp*, *S100a8*, *Cxcr2* and *Cxcl5* were stimulated in RAW264.7 cells primed with conditioned media from AN3CA cells compared to RAW264.7 cells primed with RK3E conditioned media. Increased levels of these genes in RAW264.7 cells primed with AN3CA conditioned media were suppressed when AN3CA cells were treated with dexamethasone prior to collecting conditioned media (Figure 6f). However, we did not see any differences in *Ccl9*, *Csf3r*, *Il1rn* and *Clec7a* in RAW264.7 cells cultured with conditioned media from vehicle or dexamethasone treated AN3CA cells. *S100a9* and *Ccl17* were undetectable in RAW264.7 cells. We used *Il6* as a positive control for activated NFκB signaling in RAW264.7 cells.[62] These findings indicate that NFκB signaling in EC cells results in production of inflammation-related factors that stimulate macrophages and contribute to the development of the tumor microenvironment.

DISCUSSION

TP53 mutation occurs in 80% of T2ECs.[3, 4] Recent genome-wide analysis has also confirmed high rates (81.6%) of somatic mutation in *TP53* in serous ECs.[63] Loss of CDH1 function through genetic or epigenetic mechanisms has been implicated in the progression and metastasis of numerous malignancies.[21, 64–70] Negative or reduced expression of CDH1 is one of the features of T2ECs associated with aggressive and invasive characteristics.[10, 15, 71, 72] In our model, however, mice with single gene ablation of *Trp53* or *Cdh1* in the uterus did not develop ECs, indicating that inactivation of *Trp53* or *Cdh1* alone does not contribute to tumor initiation and progression. On the other hand, loss of *Trp53* along with *Cdh1* ablation induces ECs similar to human T2ECs. We report that ablation of *Trp53* and *Cdh1* accelerates the features of neoplastic transformation in the uterus by inducing myometrial invasion, proliferation, angiogenesis, tumor dissemination, abnormal steroid hormone receptor expression and chronic inflammation.

Histological features of $Cdh1^{d/d}Trp53^{d/d}$ uteri exhibited papillary proliferation of small sized cells of the surface epithelium that have very hyperchromatic nuclei similar to T2ECs

pathogenesis, while ablation of *Trp53* and *Cdh1* did not induce well differentiated epithelial hyperplasia, which is one of the features of T1ECs. One of the key features between T1ECs and T2ECs is steroid hormone dependency. It is known that T2ECs are estrogen-independent, while T1ECs are an estrogen-dependent disease.[3, 4] Expression of ESR1 and PGR in ECs usually signifies that the tumors are well differentiated. Progestin hormone therapy has been used to slow the growth of T1ECs due to its inhibitory effects on estrogen action. However, hormone therapy does not work in T2ECs, because expression of these receptors declines in tumors that are poorly differentiated or of higher grade.[73] The present study demonstrated that ovariectomized $Cdh1^{d/d}Trp53^{d/d}$ mice developed ECs with reduced expression of ESR1 and PGR, suggesting that tumorigenesis in the uteri of $Cdh1^{d/d}Trp53^{d/d}$ mice is steroid hormone independent and associated with poorly differentiated phenotypes. In a previous study, we reported that single ablation of *Cdh1* is associated with reduced expression of steroid hormone receptors.[74] Thus, it is likely that loss of *Cdh1* promotes disruption of steroid hormone receptors that contributes to steroid hormone independence in T2ECs leading to aggressive phenotypes when cells are initiated by ablation of *Trp53*.

Because our results suggest that $Cdh1^{d/d}Trp53^{d/d}$ tumors are hormone independent ECs, we explored the etiology of tumorigenesis. Our transcriptional profiling found that most of the dysregulated genes in $Cdh1^{d/d}Trp53^{d/d}$ uteri were linked to inflammatory responses. The majority of these genes were significantly upregulated in $Cdh1^{d/d}Trp53^{d/d}$ uteri at 2-mo, and then still high at 12-mo. Further, we found evidence of activation of NFκB and STAT3 signaling in $Cdh1^{d/d}Trp53^{d/d}$ uteri at 6- and 12-mo. Thus, chronic inflammation is occurring in the uterus in the absence of *Cdh1* and *Trp53*. Tumor development is thought to depend on an interaction between initiated cells and their microenvironment.[75] Inflammation has been established as a frequent tumor promoter through alteration of the tumor microenvironment.[76] The tumor microenvironment is expected to consist of inflammatory cells (TAM and neutrophils etc) in addition to the cancer cells and their surrounding cells (cancer associated-fibroblasts, endothelial and mesenchymal cells).[52, 53, 77, 78] These diverse cells will communicate with each other by means of direct contact or cytokine and chemokine production, and act in autocrine and paracrine manners to enhance tumor progression. In the present study, we observed detectable CD68 and CD163, as well as increased levels of *Arg1* in $Cdh1^{d/d}Trp53^{d/d}$ but not in control uteri at 6- or 12-mo. CD68 and CD168 are markers of macrophages and CD163 is specific to TAMs in human cancers including ECs.[79] *Arg1* is a useful M2 marker in mice.[60, 61] Thus, our results suggest that not only classically activated macrophages, but also polarized M2 macrophages/TAMs, are involved in our model at this stage. When macrophage cells were cultured with conditioned media from EC cells, abundant chemokines, cytokines and enzymes from our microarray were expressed in the macrophage cells. The expression of these factors correlated with activation of NFκB signaling in cancer cells. Interestingly, these results were clearly recapitulated in macrophage cells that were primed in media conditioned by AN3CA cells, which lack CDH1 and harbor a mutation in *TP53*, but not by KLE cells, which have abundant CDH1 and mutated *TP53*. This implies EC cells educate recruited macrophages to become TAMs by inducing the polarization of macrophages toward to the M2 phenotype through production of factors downstream of NFκB signaling in the cancer cells themselves, and stimulate the production of chemokines, cytokines and enzymes related to chronic

inflammation by TAMs that contributes to the development of the tumor microenvironment. Although the factors derived from EC cells remain to be investigated, S100A8 and IL1B are potential candidates since both cytokines are produced by cancer cells, especially epithelial cancer cells.[80–82]

We also observed complex angiogenesis and invasion in *Cdh1*$^{d/d}$*Trp53*$^{d/d}$ uteri. Angiogenesis, a critical process in tumor progression, is associated with chronic inflammation.[83, 84] TAMs are also involved in angiogenesis in cancer.[85] While aberrant cellular invasiveness, typically accelerated by loss of CDH1, is a hallmark property of epithelial-to-mesenchymal transition (EMT), the expression of transcriptional repressors of CDH1 was not altered compared to control tissues (data not shown). Thus, any EMT-like characteristics in our model stem from direct deletion of *Cdh1* and not alteration of other signaling networks that operate upstream or in conjunction with CDH1 signaling. Further, cellular invasiveness was observed in the uteri of *Cdh1*$^{d/d}$*Trp53*$^{d/d}$ mice, but not *Cdh1*$^{d/d}$ mice. Therefore, chronic inflammation caused by loss of *Trp53* and *Cdh1* in the uterus is the suspected cause of invasive and/or EMT-like phenotypes. In support of this, the tumor inflammatory microenvironment can facilitate the breakage of the basement membrane, a process required for the invasion and migration of tumor cells.[77]

Collectively, results of the present study indicate that chronic inflammation initiated in our mouse model with *Cdh1* and *Trp53* ablation modifies the tumor microenvironment and promotes aggressive tumor development. Because elucidation of the molecular pathogenesis underlying T2ECs remains key to the development of novel therapeutic approaches, our mouse model provides valuable information on genetic, temporal and dynamic aspects of the tumor microenvironment in this cancer. However, activation of NFκB signaling is not directly induced by these gene mutations in other cancers, and they exert critical oncogenic functions most likely in cancer and immune cells within the microenvironment.[85] Therefore, the precise mechanism of NFκB signaling activated by absence of TP53 and CDH1 remains to be investigated.

MATERIALS AND METHODS

Animals and tissue collection

Mice were maintained in the vivarium at Southern Illinois University according to the institutional guidelines for the care and use of laboratory animals. B6.129-*Pgr*$^{tm2(cre)Lyd}$ (aka *Pgr*$^{cre/+}$) mice were provided by Drs. Franco DeMayo and John Lydon.[86] B6.129-*Cdh1*^{tmKem2}/J (aka *Cdh1*^{flox}, Jax #005319) and FVB.129-*Trp53*^{tm1Brn} (aka *Trp53*^{flox}, #01XC2) were obtained from the Jackson Laboratory and the Mouse Models of Human Cancers Consortium, NIH, respectively. The uteri were collected at various time points, and uterine tissues were fixed in fresh 4% paraformaldehyde in PBS at room temperature for 8–12 h and embedded in paraffin, or snap-frozen in liquid nitrogen and stored at −80 °C.

Immunohistochemical analysis

Immunolocalization of Ki67, CD31, ESR1, PGR, p-IKK, p-STAT3, CD68, CD163, COX2, iNOS, MMP9 and p-AKT was determined in cross-sections (5 μm) of paraffin-embedded

uterine sections using specific primary antibodies and a Vectastain Elite ABC Kit (Vector laboratories, Burlingame, CA, USA) or DyLight-conjugated secondary antibody (Jackson ImmunoResearch Lab, West Grove, PA, USA). Antibodies used in these analyses were: anti-CDH1 (1:120 dilution, 610181, BD Biosciences, San Jose, CA, USA), anti-Ki67 (1:200 dilution, 550609, BD Biosciences), anti-CD31 (1:100 dilution, ab28364, Abcam, Cambridge, MA, USA), anti-ESR1 (1:100 dilution, sc-542, Santa Cruz Biotechnology, Santa Cruz, CA, USA), anti-PGR (1:200 dilution, RB-9017-P0, Thermo Scientific, Rockford, IL, USA), p-IKK (1:150 dilution, 2697, Cell Signaling Technology, Danvers, MA, USA), p-STAT3 (1:50 dilution, 9145, Cell Signaling Technology), CD68 (1:300 dilution, ab955, Abcam), CD163 (1:300 dilution, ab126756, Abcam), COX2 (1:50 dilution, RM-9121, Thermo Scientific), iNOS (1:50 dilution, 610333, BD Biosciences), MMP9 (1:50 dilution, 3852, Cell Signaling Technology), and p-AKT (1:200 dilution, 3787, Cell Signaling Technology).

Microarray and qPCR analyses

Total RNA was isolated from mouse uterus using the RNeasy mini kit (Qiagen, Valencia, CA, USA). RNA quality was assessed, and then RNA probes were generated and hybridized to mouse WG-6 v2 Beadchip kit (Illumina, San Diego, CA, USA) in the Functional Genomics Core Facility of University of Illinois. Array data were processed in R (2.14.1) using the limma (3.10.2) BioConductor package.

QPCR was performed following MIQE guidelines described in Supplementary Table 2. Primers are shown in Supplementary Table 3 for mice and Supplementary Table 4 for human.

Cell culture

AN3CA, KLE, RAW 264.7 and RK3E were purchased from American Type Culture Collection (ATCC). All cells were authenticated by short tandem repeat (STR) analysis and passaged within 6-mo of receipt. Further, all cells were tested routinely for cell proliferation and BrdU incorporation as well as mycoplasma contamination, and they showed similar growth rate and negative mycoplasma during the experiment. All cells were cultured in DMEM with 10% FBS, 200 mM glutamine and penicillin/streptomycin and grown at 37 °C in a humidified 5% CO2 incubator.

Western blot analysis

Ten micrograms of total protein from the cell lysates were separated on SDS-PAGE gels and transferred to nitrocellulose membranes (Millipore Corp., Bedford, MA, USA). Membranes were blocked and incubated overnight with primary antibodies: anti-IκB (1:500 dilution, 9242, Cell Signaling Technology), anti-CDH1 (1:1000 dilution, 610181, BD Biosciences), and anti-β-actin (1:500 dilution, ab8229, Abcam). Immunoreactivity was visualized with IRDye 700 or 800 conjugated affinity-purified secondary antibodies (1:10000 dilution, Rockland Immunochemicals, Gilbertsville, PA, USA) using the Odyssey infrared imaging system (Li-COR, Lincoln, NE, USA).

Statistical analysis

Overall survival rates were determined by Kaplan-Meier analysis and P-value was determined by log-rank test using Prism4.0 (GraphPad, San Diego, CA, USA). All experimental data were subjected to one-way ANOVA and differences between individual means were tested by a Tukey multiple-range test using Prism4.0. Tests of significance were performed using the appropriate error terms according to the expectation of the mean squares for error. A P-value of 0.05 or less was considered significant. Data are presented as least-square means with standard error of the mean.

Supplementary Material

Refer to Web version on PubMed Central for supplementary material.

Acknowledgments

We thank Jenny Zadeh at the University of Illinois at Urbana-Champaign Biotechnology Center for microarray analysis. This work was supported by NIH/NCI R15CA179214 and ACS-IL 139038 (to KH), NIH/NICHD R15HD065584 (to JAM), and NIH/NICHD U54HD007495 (to FJD and JPL).

References

1. Siegel R, Ma J, Zou Z, Jemal A. Cancer statistics, 2014. CA: a cancer journal for clinicians. 2014; 64:9–29. [PubMed: 24399786]
2. Bokhman JV. Two pathogenetic types of endometrial carcinoma. Gynecologic oncology. 1983; 15:10–17. [PubMed: 6822361]
3. Lax SF. Molecular genetic pathways in various types of endometrial carcinoma: from a phenotypical to a molecular-based classification. Virchows Archiv : an international journal of pathology. 2004; 444:213–223. [PubMed: 14747944]
4. Llobet D, Pallares J, Yeramian A, Santacana M, Eritja N, Velasco A, et al. Molecular pathology of endometrial carcinoma: practical aspects from the diagnostic and therapeutic viewpoints. J Clin Pathol. 2009; 62:777–785. [PubMed: 18977806]
5. Acharya S, Hensley ML, Montag AC, Fleming GF. Rare uterine cancers. Lancet Oncol. 2005; 6:961–971. [PubMed: 16321764]
6. Goff BA. Uterine papillary serous carcinoma: what have we learned over the past quarter century? Gynecologic oncology. 2005; 98:341–343. [PubMed: 16111527]
7. Marchetti M, Vasile C, Chiarelli S. Endometrial cancer: asymptomatic endometrial findings. Characteristics of postmenopausal endometrial cancer. Eur J Gynaecol Oncol. 2005; 26:479–484. [PubMed: 16285561]
8. Di Cristofano A, Ellenson LH. Endometrial carcinoma. Annu Rev Pathol. 2007; 2:57–85. [PubMed: 18039093]
9. Horn LC, Meinel A, Handzel R, Einenkel J. Histopathology of endometrial hyperplasia and endometrial carcinoma: an update. Ann Diagn Pathol. 2007; 11:297–311. [PubMed: 17630117]
10. Samarnthai N, Hall K, Yeh IT. Molecular profiling of endometrial malignancies. Obstet Gynecol Int. 2010; 2010:162363. [PubMed: 20368795]
11. Ambros RA, Sherman ME, Zahn CM, Bitterman P, Kurman RJ. Endometrial intraepithelial carcinoma: a distinctive lesion specifically associated with tumors displaying serous differentiation. Hum Pathol. 1995; 26:1260–1267. [PubMed: 7590702]
12. Soong R, Knowles S, Williams KE, Hammond IG, Wysocki SJ, Iacopetta BJ. Overexpression of p53 protein is an independent prognostic indicator in human endometrial carcinoma. British journal of cancer. 1996; 74:562–567. [PubMed: 8761370]

13. Vleminckx K, Kemler R. Cadherins and tissue formation: integrating adhesion and signaling. BioEssays : news and reviews in molecular, cellular and developmental biology. 1999; 21:211–220.
14. Huszar M, Pfeifer M, Schirmer U, Kiefel H, Konecny GE, Ben-Arie A, et al. Up-regulation of L1CAM is linked to loss of hormone receptors and E-cadherin in aggressive subtypes of endometrial carcinomas. J Pathol. 2010; 220:551–561. [PubMed: 20077528]
15. Koyuncuoglu M, Okyay E, Saatli B, Olgan S, Akin M, Saygili U. Tumor budding and E-Cadherin expression in endometrial carcinoma: are they prognostic factors in endometrial cancer? Gynecologic oncology. 2012; 125:208–213. [PubMed: 22198340]
16. Moll R, Mitze M, Frixen UH, Birchmeier W. Differential loss of E-cadherin expression in infiltrating ductal and lobular breast carcinomas. Am J Pathol. 1993; 143:1731–1742. [PubMed: 8256859]
17. Wu ZY, Zhan WH, Li JH, He YL, Wang JP, Lan P, et al. Expression of E-cadherin in gastric carcinoma and its correlation with lymph node micrometastasis. World journal of gastroenterology : WJG. 2005; 11:3139–3143. [PubMed: 15918205]
18. Bremnes RM, Veve R, Hirsch FR, Franklin WA. The E-cadherin cell-cell adhesion complex and lung cancer invasion, metastasis, and prognosis. Lung cancer. 2002; 36:115–124. [PubMed: 11955645]
19. De Marzo AM, Knudsen B, Chan-Tack K, Epstein JI. E-cadherin expression as a marker of tumor aggressiveness in routinely processed radical prostatectomy specimens. Urology. 1999; 53:707–713. [PubMed: 10197845]
20. Oka H, Shiozaki H, Kobayashi K, Inoue M, Tahara H, Kobayashi T, et al. Expression of E-cadherin cell adhesion molecules in human breast cancer tissues and its relationship to metastasis. Cancer research. 1993; 53:1696–1701. [PubMed: 8453644]
21. Perl AK, Wilgenbus P, Dahl U, Semb H, Christofori G. A causal role for E-cadherin in the transition from adenoma to carcinoma. Nature. 1998; 392:190–193. [PubMed: 9515965]
22. Takeichi M. Cadherins in cancer: implications for invasion and metastasis. Curr Opin Cell Biol. 1993; 5:806–811. [PubMed: 8240824]
23. Donehower LA, Harvey M, Slagle BL, McArthur MJ, Montgomery CA Jr, Butel JS, et al. Mice deficient for p53 are developmentally normal but susceptible to spontaneous tumours. Nature. 1992; 356:215–221. [PubMed: 1552940]
24. Harvey M, McArthur MJ, Montgomery CA Jr, Bradley A, Donehower LA. Genetic background alters the spectrum of tumors that develop in p53-deficient mice. FASEB journal : official publication of the Federation of American Societies for Experimental Biology. 1993; 7:938–943. [PubMed: 8344491]
25. Jacks T, Remington L, Williams BO, Schmitt EM, Halachmi S, Bronson RT, et al. Tumor spectrum analysis in p53-mutant mice. Current biology : CB. 1994; 4:1–7. [PubMed: 7922305]
26. Franco HL, Jeong JW, Tsai SY, Lydon JP, DeMayo FJ. In vivo analysis of progesterone receptor action in the uterus during embryo implantation. Semin Cell Dev Biol. 2008; 19:178–186. [PubMed: 18280760]
27. Daikoku T, Hirota Y, Tranguch S, Joshi AR, DeMayo FJ, Lydon JP, et al. Conditional loss of uterine Pten unfailingly and rapidly induces endometrial cancer in mice. Cancer research. 2008; 68:5619–5627. [PubMed: 18632614]
28. Kim TH, Franco HL, Jung SY, Qin J, Broaddus RR, Lydon JP, et al. The synergistic effect of Mig-6 and Pten ablation on endometrial cancer development and progression. Oncogene. 2010; 29:3770–3780. [PubMed: 20418913]
29. Reardon SN, King ML, MacLean JA 2nd, Mann JL, DeMayo FJ, Lydon JP, et al. CDH1 is essential for endometrial differentiation, gland development, and adult function in the mouse uterus. Biology of reproduction. 2012; 86:141, 141–110. [PubMed: 22378759]
30. Boussadia O, Kutsch S, Hierholzer A, Delmas V, Kemler R. E-cadherin is a survival factor for the lactating mouse mammary gland. Mech Dev. 2002; 115:53–62. [PubMed: 12049767]
31. Derksen PW, Braumuller TM, van der Burg E, Hornsveld M, Mesman E, Wesseling J, et al. Mammary-specific inactivation of E-cadherin and p53 impairs functional gland development and

leads to pleomorphic invasive lobular carcinoma in mice. Disease models & mechanisms. 2011; 4:347–358. [PubMed: 21282721]

32. Derksen PW, Liu X, Saridin F, van der Gulden H, Zevenhoven J, Evers B, et al. Somatic inactivation of E-cadherin and p53 in mice leads to metastatic lobular mammary carcinoma through induction of anoikis resistance and angiogenesis. Cancer cell. 2006; 10:437–449. [PubMed: 17097565]
33. Shimada S, Mimata A, Sekine M, Mogushi K, Akiyama Y, Fukamachi H, et al. Synergistic tumour suppressor activity of E-cadherin and p53 in a conditional mouse model for metastatic diffuse-type gastric cancer. Gut. 2012; 61:344–353. [PubMed: 21865403]
34. Larue L, Ohsugi M, Hirchenhain J, Kemler R. E-cadherin null mutant embryos fail to form a trophectoderm epithelium. Proceedings of the National Academy of Sciences of the United States of America. 1994; 91:8263–8267. [PubMed: 8058792]
35. Riethmacher D, Brinkmann V, Birchmeier C. A targeted mutation in the mouse E-cadherin gene results in defective preimplantation development. Proceedings of the National Academy of Sciences of the United States of America. 1995; 92:855–859. [PubMed: 7846066]
36. Sherman ME, Bitterman P, Rosenshein NB, Delgado G, Kurman RJ. Uterine serous carcinoma. A morphologically diverse neoplasm with unifying clinicopathologic features. Am J Surg Pathol. 1992; 16:600–610. [PubMed: 1599038]
37. Bansal N, Yendluri V, Wenham RM. The molecular biology of endometrial cancers and the implications for pathogenesis, classification, and targeted therapies. Cancer control : journal of the Moffitt Cancer Center. 2009; 16:8–13. [PubMed: 19078924]
38. Tuominen VJ, Ruotoistenmaki S, Viitanen A, Jumppanen M, Isola J. ImmunoRatio: a publicly available web application for quantitative image analysis of estrogen receptor (ER), progesterone receptor (PR), and Ki-67. Breast cancer research : BCR. 2010; 12:R56. [PubMed: 20663194]
39. Kim MY, Oskarsson T, Acharyya S, Nguyen DX, Zhang XH, Norton L, et al. Tumor self-seeding by circulating cancer cells. Cell. 2009; 139:1315–1326. [PubMed: 20064377]
40. Klein CA. Parallel progression of primary tumours and metastases. Nature reviews Cancer. 2009; 9:302–312.
41. Norton L, Massague J. Is cancer a disease of self-seeding? Nature medicine. 2006; 12:875–878.
42. Riethmuller G, Klein CA. Early cancer cell dissemination and late metastatic relapse: clinical reflections and biological approaches to the dormancy problem in patients. Seminars in cancer biology. 2001; 11:307–311. [PubMed: 11513566]
43. Dennis G Jr, Sherman BT, Hosack DA, Yang J, Gao W, Lane HC, et al. DAVID: Database for Annotation, Visualization, and Integrated Discovery. Genome biology. 2003; 4:P3. [PubMed: 12734009]
44. Huang da W, Sherman BT, Lempicki RA. Systematic and integrative analysis of large gene lists using DAVID bioinformatics resources. Nature protocols. 2009; 4:44–57. [PubMed: 19131956]
45. Subramanian A, Tamayo P, Mootha VK, Mukherjee S, Ebert BL, Gillette MA, et al. Gene set enrichment analysis: a knowledge-based approach for interpreting genome-wide expression profiles. Proceedings of the National Academy of Sciences of the United States of America. 2005; 102:15545–15550. [PubMed: 16199517]
46. Maxwell GL, Chandramouli GV, Dainty L, Litzi TJ, Berchuck A, Barrett JC, et al. Microarray analysis of endometrial carcinomas and mixed mullerian tumors reveals distinct gene expression profiles associated with different histologic types of uterine cancer. Clinical cancer research : an official journal of the American Association for Cancer Research. 2005; 11:4056–4066. [PubMed: 15930340]
47. Moreno-Bueno G, Sanchez-Estevez C, Cassia R, Rodriguez-Perales S, Diaz-Uriarte R, Dominguez O, et al. Differential gene expression profile in endometrioid and nonendometrioid endometrial carcinoma: STK15 is frequently overexpressed and amplified in nonendometrioid carcinomas. Cancer research. 2003; 63:5697–5702. [PubMed: 14522886]
48. Risinger JI, Maxwell GL, Chandramouli GV, Jazaeri A, Aprelikova O, Patterson T, et al. Microarray analysis reveals distinct gene expression profiles among different histologic types of endometrial cancer. Cancer research. 2003; 63:6–11. [PubMed: 12517768]

49. Santin AD, Zhan F, Cane S, Bellone S, Palmieri M, Thomas M, et al. Gene expression fingerprint of uterine serous papillary carcinoma: identification of novel molecular markers for uterine serous cancer diagnosis and therapy. British journal of cancer. 2005; 92:1561–1573. [PubMed: 15785748]
50. Bollrath J, Greten FR. IKK/NF-kappaB and STAT3 pathways: central signalling hubs in inflammation-mediated tumour promotion and metastasis. EMBO reports. 2009; 10:1314–1319. [PubMed: 19893576]
51. Lorusso G, Ruegg C. The tumor microenvironment and its contribution to tumor evolution toward metastasis. Histochemistry and cell biology. 2008; 130:1091–1103. [PubMed: 18987874]
52. Lu H, Ouyang W, Huang C. Inflammation, a key event in cancer development. Molecular cancer research : MCR. 2006; 4:221–233. [PubMed: 16603636]
53. Wu Y, Zhou BP. Inflammation: a driving force speeds cancer metastasis. Cell cycle. 2009; 8:3267–3273. [PubMed: 19770594]
54. Karin M, Cao Y, Greten FR, Li ZW. NF-kappaB in cancer: from innocent bystander to major culprit. Nature reviews Cancer. 2002; 2:301–310. [PubMed: 12001991]
55. Li N, Grivennikov SI, Karin M. The unholy trinity: inflammation, cytokines, and STAT3 shape the cancer microenvironment. Cancer cell. 2011; 19:429–431. [PubMed: 21481782]
56. Yu H, Pardoll D, Jove R. STATs in cancer inflammation and immunity: a leading role for STAT3. Nature reviews Cancer. 2009; 9:798–809. [PubMed: 19851315]
57. Mantovani A, Sozzani S, Locati M, Allavena P, Sica A. Macrophage polarization: tumor-associated macrophages as a paradigm for polarized M2 mononuclear phagocytes. Trends in immunology. 2002; 23:549–555. [PubMed: 12401408]
58. Sica A, Mantovani A. Macrophage plasticity and polarization: in vivo veritas. The Journal of clinical investigation. 2012; 122:787–795. [PubMed: 22378047]
59. Mazieres J, Brugger W, Cappuzzo F, Middel P, Frosch A, Bara I, et al. Evaluation of EGFR protein expression by immunohistochemistry using H-score and the magnification rule: re-analysis of the SATURN study. Lung cancer. 2013; 82:231–237. [PubMed: 23972450]
60. Raes G, Van den Bergh R, De Baetselier P, Ghassabeh GH, Scotton C, Locati M, et al. Arginase-1 and Ym1 are markers for murine, but not human, alternatively activated myeloid cells. Journal of immunology. 2005; 174:6561. author reply 6561–6562.
61. Scotton CJ, Martinez FO, Smelt MJ, Sironi M, Locati M, Mantovani A, et al. Transcriptional profiling reveals complex regulation of the monocyte IL-1 beta system by IL-13. Journal of immunology. 2005; 174:834–845.
62. Medvedev AE, Blanco JC, Qureshi N, Vogel SN. Limited role of ceramide in lipopolysaccharide-mediated mitogen-activated protein kinase activation, transcription factor induction, and cytokine release. The Journal of biological chemistry. 1999; 274:9342–9350. [PubMed: 10092612]
63. Kuhn E, Wu RC, Guan B, Wu G, Zhang J, Wang Y, et al. Identification of molecular pathway aberrations in uterine serous carcinoma by genome-wide analyses. Journal of the National Cancer Institute. 2012; 104:1503–1513. [PubMed: 22923510]
64. Berx G, Becker KF, Hofler H, van Roy F. Mutations of the human E-cadherin (CDH1) gene. Human mutation. 1998; 12:226–237. [PubMed: 9744472]
65. Cleton-Jansen AM, Moerland EW, Kuipers-Dijkshoorn NJ, Callen DF, Sutherland GR, Hansen B, et al. At least two different regions are involved in allelic imbalance on chromosome arm 16q in breast cancer. Genes, chromosomes & cancer. 1994; 9:101–107. [PubMed: 7513539]
66. Comijn J, Berx G, Vermassen P, Verschueren K, van Grunsven L, Bruyneel E, et al. The two-handed E box binding zinc finger protein SIP1 downregulates E-cadherin and induces invasion. Mol Cell. 2001; 7:1267–1278. [PubMed: 11430829]
67. Frixen UH, Behrens J, Sachs M, Eberle G, Voss B, Warda A, et al. E-cadherin-mediated cell-cell adhesion prevents invasiveness of human carcinoma cells. The Journal of cell biology. 1991; 113:173–185. [PubMed: 2007622]
68. Graff JR, Herman JG, Lapidus RG, Chopra H, Xu R, Jarrard DF, et al. E-cadherin expression is silenced by DNA hypermethylation in human breast and prostate carcinomas. Cancer research. 1995; 55:5195–5199. [PubMed: 7585573]

69. Oda T, Kanai Y, Oyama T, Yoshiura K, Shimoyama Y, Birchmeier W, et al. E-cadherin gene mutations in human gastric carcinoma cell lines. Proceedings of the National Academy of Sciences of the United States of America. 1994; 91:1858–1862. [PubMed: 8127895]
70. Vleminckx K, Vakaet L Jr, Mareel M, Fiers W, van Roy F. Genetic manipulation of E-cadherin expression by epithelial tumor cells reveals an invasion suppressor role. Cell. 1991; 66:107–119. [PubMed: 2070412]
71. Holcomb K, Delatorre R, Pedemonte B, McLeod C, Anderson L, Chambers J. E-cadherin expression in endometrioid, papillary serous, and clear cell carcinoma of the endometrium. Obstetrics and gynecology. 2002; 100:1290–1295. [PubMed: 12468176]
72. Shaco-Levy R, Sharabi S, Piura B, Sion-Vardy N. MMP-2, TIMP-1, E-cadherin, and beta-catenin expression in endometrial serous carcinoma compared with low-grade endometrial endometrioid carcinoma and proliferative endometrium. Acta obstetricia et gynecologica Scandinavica. 2008; 87:868–874. [PubMed: 18607832]
73. Kim JJ, Kurita T, Bulun SE. Progesterone action in endometrial cancer, endometriosis, uterine fibroids, and breast cancer. Endocrine reviews. 2013; 34:130–162. [PubMed: 23303565]
74. Lindberg ME, Stodden GR, King ML, MacLean JA 2nd, Mann JL, DeMayo FJ, et al. Loss of CDH1 and pten accelerates cellular invasiveness and angiogenesis in the mouse uterus. Biology of reproduction. 2013; 89:8. [PubMed: 23740945]
75. Albini A, Sporn MB. The tumour microenvironment as a target for chemoprevention. Nature reviews Cancer. 2007; 7:139–147. [PubMed: 17218951]
76. Karin M. Nuclear factor-kappaB in cancer development and progression. Nature. 2006; 441:431–436. [PubMed: 16724054]
77. Coussens LM, Werb Z. Inflammation and cancer. Nature. 2002; 420:860–867. [PubMed: 12490959]
78. Grivennikov SI, Greten FR, Karin M. Immunity, inflammation, and cancer. Cell. 2010; 140:883–899. [PubMed: 20303878]
79. Heusinkveld M, van der Burg SH. Identification and manipulation of tumor associated macrophages in human cancers. Journal of translational medicine. 2011; 9:216. [PubMed: 22176642]
80. Hermani A, De Servi B, Medunjanin S, Tessier PA, Mayer D. S100A8 and S100A9 activate MAP kinase and NF-kappaB signaling pathways and trigger translocation of RAGE in human prostate cancer cells. Experimental cell research. 2006; 312:184–197. [PubMed: 16297907]
81. Moon A, Yong HY, Song JI, Cukovic D, Salagrama S, Kaplan D, et al. Global gene expression profiling unveils S100A8/A9 as candidate markers in H-ras-mediated human breast epithelial cell invasion. Molecular cancer research : MCR. 2008; 6:1544–1553. [PubMed: 18922970]
82. Reed JR, Leon RP, Hall MK, Schwertfeger KL. Interleukin-1beta and fibroblast growth factor receptor 1 cooperate to induce cyclooxygenase-2 during early mammary tumourigenesis. Breast cancer research : BCR. 2009; 11:R21. [PubMed: 19393083]
83. De Palma M, Venneri MA, Galli R, Sergi Sergi L, Politi LS, Sampaolesi M, et al. Tie2 identifies a hematopoietic lineage of proangiogenic monocytes required for tumor vessel formation and a mesenchymal population of pericyte progenitors. Cancer cell. 2005; 8:211–226. [PubMed: 16169466]
84. Lin EY, Pollard JW. Role of infiltrated leucocytes in tumour growth and spread. British journal of cancer. 2004; 90:2053–2058. [PubMed: 15164120]
85. He G, Karin M. NF-kappaB and STAT3 - key players in liver inflammation and cancer. Cell research. 2011; 21:159–168. [PubMed: 21187858]
86. Soyal SM, Mukherjee A, Lee KY, Li J, Li H, DeMayo FJ, et al. Cre-mediated recombination in cell lineages that express the progesterone receptor. Genesis. 2005; 41:58–66. [PubMed: 15682389]

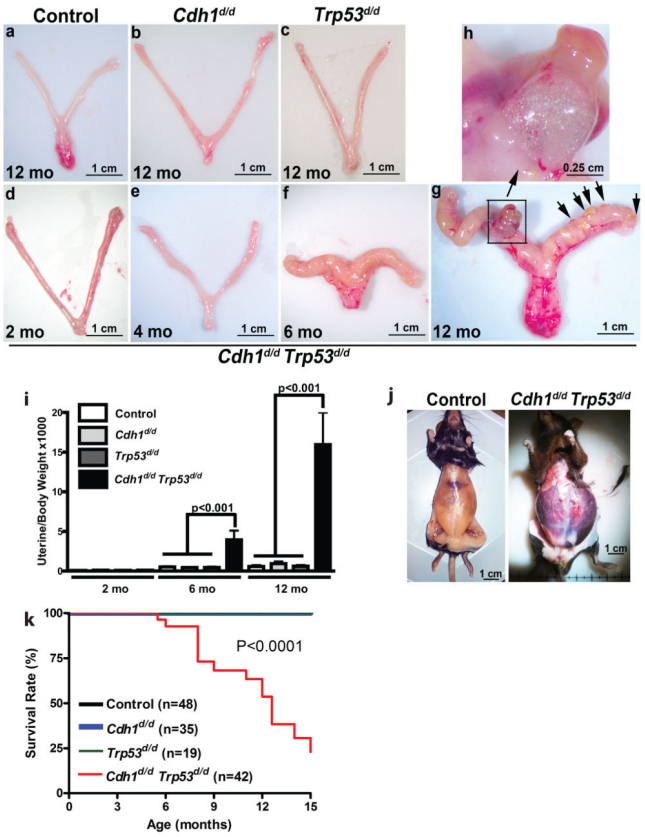

Figure 1.

Development of endometrial cancer in *Cdh1*$^{d/d}$*Trp53*$^{d/d}$ mice. Gross uterine morphology of (a) control, (b) *Cdh1*$^{d/d}$, (c) *Trp53*$^{d/d}$ and (d–h) *Cdh1*$^{d/d}$*Trp53*$^{d/d}$ mice at 2, 4, 6 and 12 months of age. (g, h) *Cdh1*$^{d/d}$*Trp53*$^{d/d}$ mice developed tumors that had expanded outside of the uterus (arrows and high magnification (h)) at 12 months of age. (i) The ratio of uterine weight to body weight in control, *Cdh1*$^{d/d}$, *Trp53*$^{d/d}$ and *Cdh1*$^{d/d}$*Trp53*$^{d/d}$ mice at 2, 6 and 12 months of age. (j) Ascites fluid accumulation was observed in *Cdh1*$^{d/d}$*Trp53*$^{d/d}$ mice (4 of 15 mice) starting around 10 months of age. (k) Overall survival rate for control, *Cdh1*$^{d/d}$, *Trp53*$^{d/d}$ and *Cdh1*$^{d/d}$*Trp53*$^{d/d}$ mice was performed by Kaplan-Meier analysis to assess whether ablation of *Cdh1* and *Trp53* is associated with short lifespan (P<0.0001). All mice were monitored for any sign of sickness. We sacrificed mice with any sign of sickness or discomfort, and the day of sacrifice was recorded.

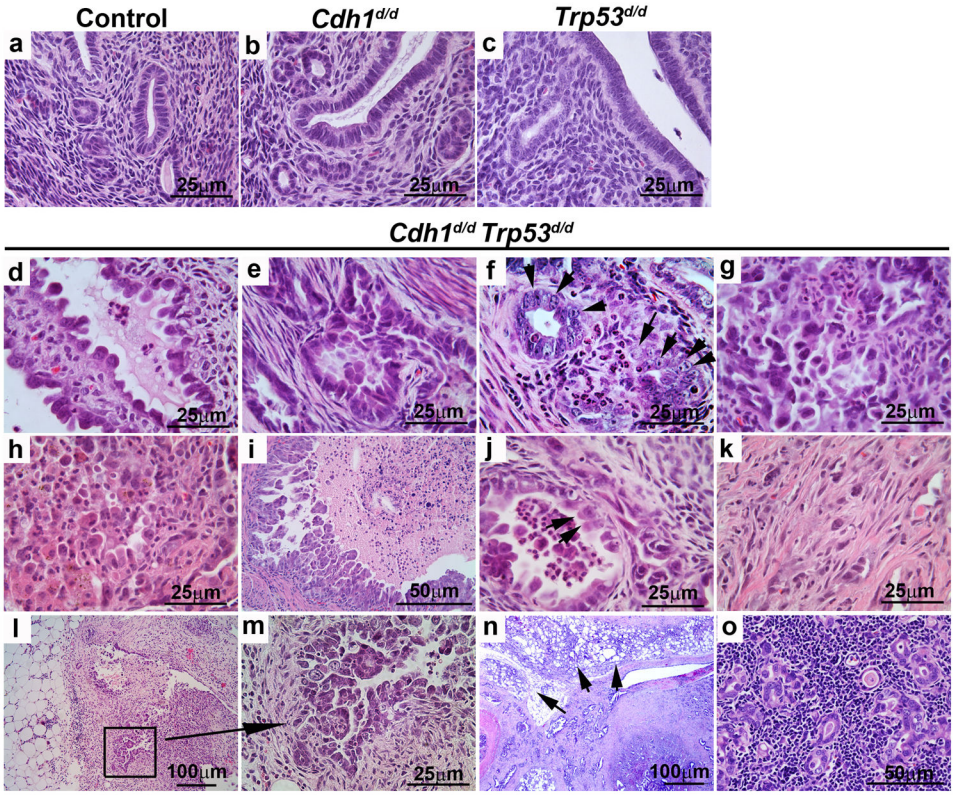

Figure 2.

Uterine histology from mice with ablation of *Cdh1* and/or *Trp53*. Tissues were stained using hematoxylin and eosin. Uterine histology of (a) control, (b) $Cdh1^{d/d}$ and (c) $Trp53^{d/d}$ mice at 12 months of age, and $Cdh1^{d/d}Trp53^{d/d}$ mice at 2 (d, e), 6 (f, g) and 12 (h–k) months of age. (d) Cellular budding like papillae. (e) Myometrial invasion. (f) Arrows point to atypical cell with large nucleus. (g, h) Representative areas of tumor showing high-grade features. (i) Papillary differentiation. (j) Arrows point to hobnailing. (k) Sarcomatous differentiation. Tumor dissemination in $Cdh1^{d/d}Trp53^{d/d}$ mice at 12 months of age into the peritoneal cavity (fat pad, (l, m)), the mesentery (n), and abdominal lymph nodes (o).

a

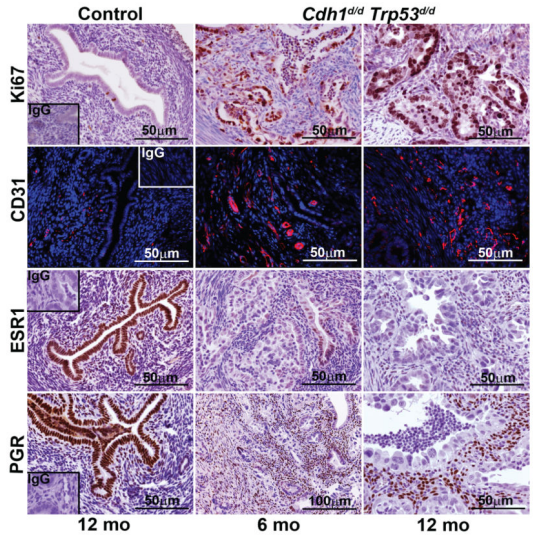

b

12 mo	%	Control	*Cdh1* $^{d/d}$ *Trp53* $^{d/d}$
	Ki67	3.7 ± 0.5	32.2 ± 4.3 *

* P<0.01 vs Control

% of Ki67 positive cells / total cells / 0.02mm^2

12 mo	Cell numbers	Control	*Cdh1* $^{d/d}$ *Trp53* $^{d/d}$
	CD31	6.9 ± 0.6	24.9 ± 4.5 *

Cell numbers of CD31 positive cells / 0.02mm^2

12 mo	%	Control	*Cdh1* $^{d/d}$ *Trp53* $^{d/d}$
ESR1	Epithelium	99.1 ± 0.5	47.1 ± 5.1 *
	Stroma	55.2 ± 9.7	42.9 ± 5.7
PGR	Epithelium	98.1 ± 0.8	32.0 ± 5.0 *
	Stroma	19.5 ± 5.9	61.7 ± 3.9 *

% of ESR1 or PGR positive cells / total cells / 0.02mm^2

Figure 3.

The effect of *Cdh1* and *Trp53* ablation on proliferation, angiogenesis and steroid hormone receptors. (a) Immunoreactive Ki67 (MKI67) as a marker of cell proliferation, CD31 (PECAM1) as an endothelial cell marker, and steroid hormone receptors (ESR1 and PGR) were detected in the uteri of control and *Cdh1*$^{d/d}$*Trp53*$^{d/d}$ mice at 6 and 12 months of age. (b) Semiquantitatively scored Ki67 by ImmunoRatio, and CD31 by positively stained cell numbers. Cell specific ESR1 and PGR positive cells were counted and the percentage (positive cells/total cells) is shown. ImmunoRatio calculates the percentage of positively stained nuclear cells/total cells.

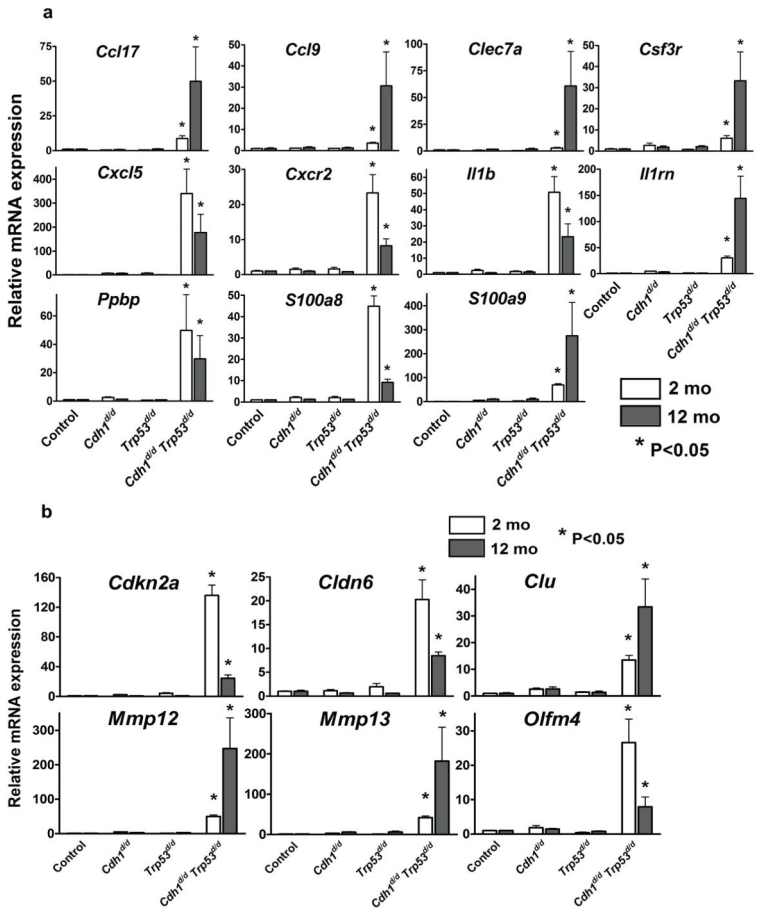

Figure 4.

The effect of *Cdh1* and/or *Trp53* ablation on gene transcripts. Specific genes identified by microarray analysis were analyzed by qPCR to confirm their gene transcripts in the uteri of control, $Cdh1^{d/d}$, $Trp53^{d/d}$ and $Cdh1^{d/d}Trp53^{d/d}$ mice at 2 and 12 months of age. The genes are related to inflammatory responses (a) and others (b). The results were normalized against *Gapdh*. * P<0.05 vs control.

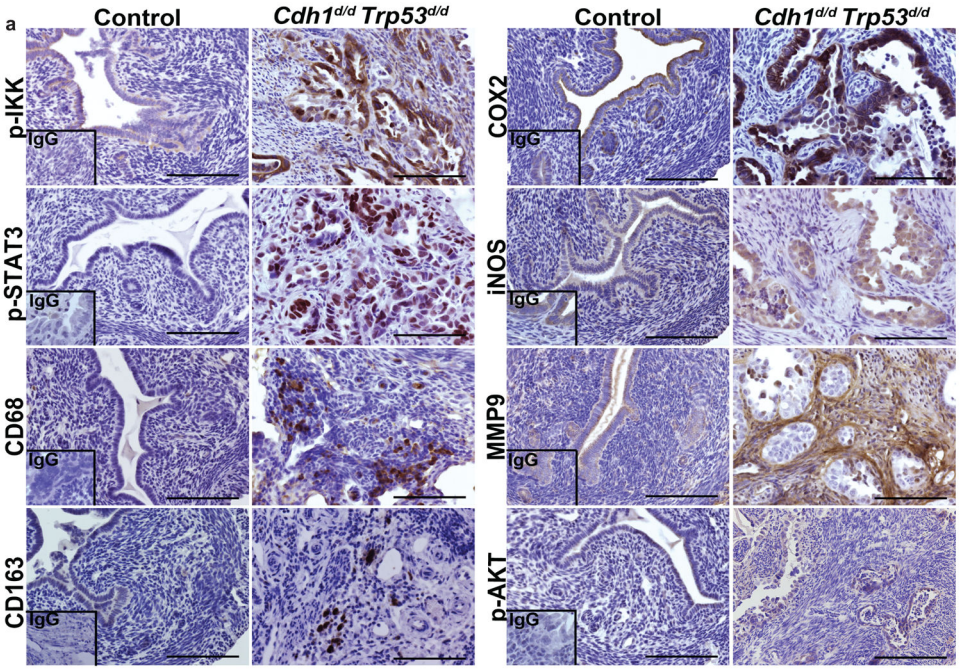

b

* P<0.01 vs Control

H-socre	Control	*Cdh1* $^{d/d}$ *Trp53* $^{d/d}$
p-IKK	12.5 ± 1.7	100.5 ± 8.4 *
COX2	82.5 ± 7.5	174.0 ± 26.4 *
iNOS	27.1 ± 4.9	138.9 ± 22.2 *
MMP9	78.6 ± 16.0	269.4 ± 6.1 *
p-AKT	0	0

%	Control	*Cdh1* $^{d/d}$ *Trp53* $^{d/d}$
p-STAT3	4.9 ± 0.8	22.7 ± 1.5 *

% of p-STAT3 positive cells / total cells / 0.02mm^2

Cell numbers	Control	*Cdh1* $^{d/d}$ *Trp53* $^{d/d}$
CD68	1.8 ± 0.5	35.1 ± 6.2 *
CD163	0.9 ± 0.3	14.0 ± 1.6 *

Cell numbers of CD68 or CD163 positive cells / 0.02mm^2

c

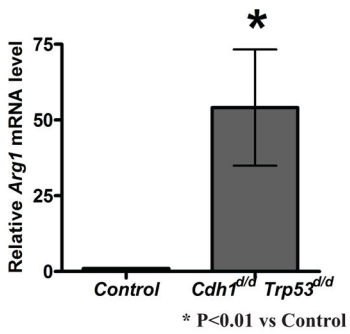

Figure 5.

The effect of *Cdh1* and/or *Trp53* ablation on inflammation. (a) Immunolocalization of p-IKK, p-STAT3, tumor associated macrophage markers (CD68 and CD163), COX2, iNOS, MMP9 and p-AKT in the uteri of control and *Cdh1*$^{d/d}$*Trp53*$^{d/d}$ mice at 12 months of age. Scale bars = 50 μm. (b) Semiquantitatively scored p-IKK, COX2, iNOS, MMP9 and p-AKT by H-score analysis, p-STAT3 by ImmunoRatio, CD68 and CD163 by positively stained cell numbers. ImmunoRatio calculates the percentage of positively stained nuclear cells/total cells. (c) QPCR analysis of *Arg1* normalized to *Gapdh* in the uteri of control and *Cdh1*$^{d/d}$*Trp53*$^{d/d}$ mice.

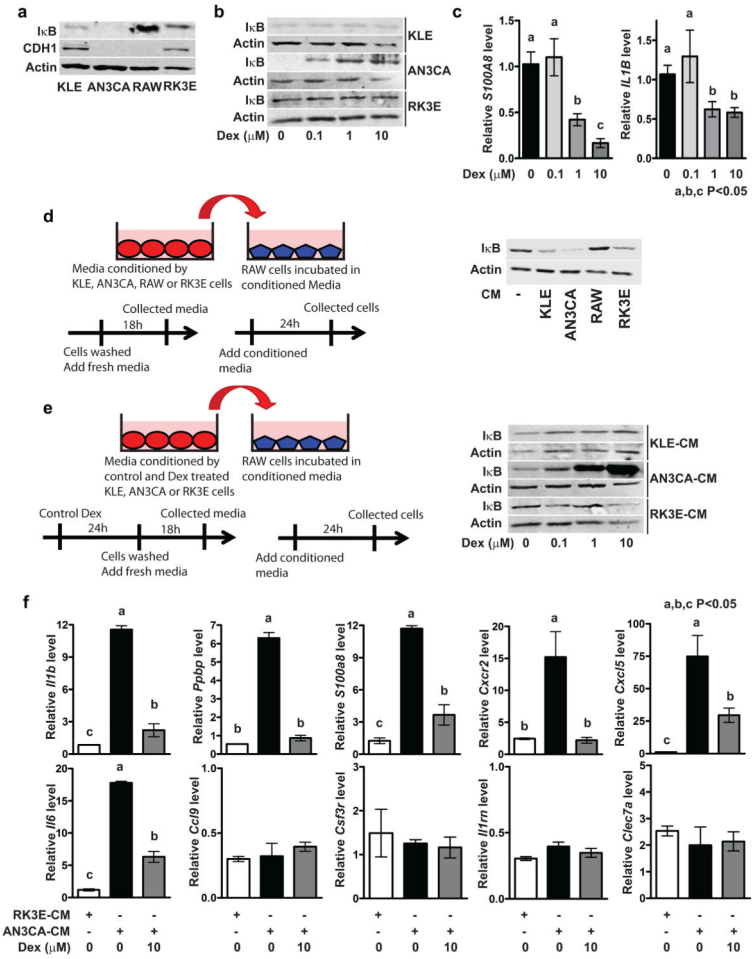

Figure 6.

Factors derived from endometrial cancer cells promote the ability of macrophages to stimulate inflammation. (a) IκB and CDH1 were determined in type II endometrial cancer cells (KLE and AN3CA), mouse macrophage cells (RAW 264.7), and rat kidney epithelial cells (RK3E) by western blot. (b) The levels of IκB protein were shown in KLE, AN3CA and RK3E cells treated with dexamethasone (0, 0.1, 1 or 10 μM) for 24 h. (c) Relative mRNA levels (*S100A8* and *IL1B*) were analyzed in AN3CA cells treated with dexamethasone (0, 0.1, 1 or 10 μM) for 24 h. The results of AN3CA cells were only shown as IkB was dexamethasone-responsive in these cells. (d) IκB protein was determined in RAW 264.7 cells primed in media conditioned by KLE, AN3CA, RAW or RK3E cells. Conditioned media (CM) were collected 18 h after the addition of fresh media. RAW 264.7 cells were cultured with conditioned media for 24 h and collected for further analysis. (e) The level of IκB protein were shown in RAW 264.7 cells primed in media conditioned by KLE, AN3CA or RK3E cells that were treated with dexamethasone (0, 0.1, 1 or 10 μM). Cells were treated with dexamethasone for 24 h, washed with PBS, and changed to fresh, drug-free media. Conditioned media were collected 18 h after the addition of fresh media. RAW 264.7 cells were cultured with conditioned media for 24 h and collected for further

analysis. (f) Relative mRNA levels shown in Figure 4a were analyzed in RAW 264.7 cells primed in media conditioned by RK3E or vehicle/dexamethasone treated-AN3CA cells.